


RESEARCH

Open Access



# Bacterial network for precise plant stress detection and enhanced crop resilience

Shakeel Ahmed<sup>1,2</sup>, Syed Muhammad Zaigham Abbas Naqvi<sup>1,2</sup>, Muhammad Awais<sup>1,2</sup>, Yongzhe Ren<sup>3,4</sup>, Hao Zhang<sup>1,2</sup>, Junfeng Wu<sup>1,2</sup>, Linze Li<sup>1,2</sup>, Vijaya Raghavan<sup>5</sup> and Jiandong Hu<sup>1,2,4\*</sup> 

\*Correspondence:  
jdhu@henau.edu.cn

<sup>1</sup> College of Mechanical and Electrical Engineering, Henan Agricultural University, Zhengzhou 450002, China

<sup>2</sup> Henan International Joint Laboratory of Laser Technology in Agriculture Sciences, Zhengzhou 450002, China

<sup>3</sup> College of Agronomy, Henan Agricultural University, Zhengzhou 450002, China

<sup>4</sup> State Key Laboratory of Wheat and Maize Crop Science, Zhengzhou 450002, China

<sup>5</sup> Department of Bioresource Engineering, Faculty of Agriculture and Environmental Studies, McGill University, Sainte-Anne-de-Bellevue, QC H9X 3V9, Canada

## Abstract

Understanding plant hormonal responses to stress and their transport dynamics remains challenging, limiting advancements in enhancing plant resilience. Our study presents a novel approach that utilizes genetically engineered bacteria (GEB) as molecular transceivers within plants, aiming to develop revolutionary agricultural biosensors. We focus on abscisic acid (ABA), a key hormone for plant growth and stress response. We propose using *Escherichia coli* (*E. coli*) engineered with PYR1-derived receptors that exhibit high affinity for ABA, triggering a bioluminescent response. Simulations investigate the detection time for ABA, bacterial diffusion within plant roots, advection effects through shoots, and chemotaxis in response to attractant gradients in leaves. Results indicate that higher ABA concentrations correlate with shorter response times, with an average of 431.52 s based on bioluminescence. The average internalization time for bacteria through a plant root area of 2  $\mu\text{m}^2$  during the rhizophagy process is estimated at 1220.12 s. Simulations also assess bacterial movement through shoots, the impact of advection, and chemotactic responses. These findings highlight the complex interplay between plant signaling and microbial communities, validating the efficacy of our bacterial-based sensor approach and opening new avenues for agricultural biosensor technology.

**Keywords:** Bacterial-based sensor, Molecular communication, Abscisic acid, Mathematical modeling, Simulations, Engineered *E. coli*-PYR1 bacteria

## Introduction

Plants have the natural ability to sense their surrounding environment [1], commonly known as stress. Stress can be biotic or abiotic and commonly coexist in nature and can be brought on by a wide range of conditions, including heat, cold, toxicity, drought, flooding, and damage from pathogens and predators, as well as by photosynthesis [2]. Plants respond uniquely to different stresses, resulting in a complex signaling network that controls and mediates their biosensory systems. In the literature, signaling refers to the production of various chemicals for molecular communication, initiating multiple activities inside and outside the plant [3]. Plants use hormones as signaling molecules to control internal activities and transfer stress responses between different parts [4].



© The Author(s) 2025. **Open Access** This article is licensed under a Creative Commons Attribution-NonCommercial-NoDerivatives 4.0 International License, which permits any non-commercial use, sharing, distribution and reproduction in any medium or format, as long as you give appropriate credit to the original author(s) and the source, provide a link to the Creative Commons licence, and indicate if you modified the licensed material. You do not have permission under this licence to share adapted material derived from this article or parts of it. The images or other third party material in this article are included in the article's Creative Commons licence, unless indicated otherwise in a credit line to the material. If material is not included in the article's Creative Commons licence and your intended use is not permitted by statutory regulation or exceeds the permitted use, you will need to obtain permission directly from the copyright holder. To view a copy of this licence, visit <http://creativecommons.org/licenses/by-nc-nd/4.0/>.

Hormones like ethylene, salicylic acid, and jasmonic acid play a vital role in responding to biotic stress. In contrast, abscisic acid (ABA) is critical in maintaining seed dormancy, preventing germination, regulating growth, stomatal closure, fruit abscission, and mediation of stress responses [5]. PYR1, a member of the PYR/PYL/RCAR (Pyrabactin resistance, Pyrabactin resistance-like, and Regulatory Component of ABA Receptors) family, functions as an ABA receptor, crucial for perceiving ABA during biotic stress. It upregulates transcriptionally and activates downstream signaling via ABA-activated SnRK2 (SNF1-Related protein kinase 2) protein kinases. PYR/PYL/RCAR receptors detect ABA intracellularly, forming ternary complexes with PP2Cs (Protein Phosphatase 2C) and SnRK2s to initiate ABA signaling. PYLs, PP2Cs, and SnRK2s are the core components of this pathway [6] presented in Fig. 1.

Molecular signaling in living cells, particularly in plants, has garnered significant attention for uncovering natural communication principles and advancing nano-networking techniques in agriculture. The interdisciplinary field of Molecular Communication (MC) formalizes this concept by exploring how molecules, cells, or bacteria can function as precise nanoscale transmitters and receivers of information [7–9]. Synthesizing, emitting, accumulating, and transforming biological responses are all accomplished through a mathematize biochemical mechanism in MC [10]. This interdisciplinary study harmonizes signals with biological systems for efficient, low-energy dissemination, suggesting that all living things can be seen as nanomachines. Bacterial-based research, using genetically engineered bacteria (GEB) for detection purposes, paves the way for advancements in nano communication and bacteria as signal transceivers [11–13].

Monitoring abscisic acid (ABA) levels is vital for identifying stress and enabling timely interventions to boost resilience and productivity. Researchers focus on controlling hormone action to improve stress tolerance and crop quality [14–16]. Several detection techniques have been developed, including surface-enhanced Raman spectroscopy (SERS) [17], laser-induced breakdown spectroscopy (LIBS) [18], and localized surface plasmon resonance [19] developed to investigate plant diseases, the impact of chemical sprays, the detection/behavior of plant hormones, and their role in plant growth through the analysis. For instance, Raman spectroscopy efficiently detects nutritional stress in plant vascular tissue [20]. Furthermore, a SERS substrate has been developed for detecting ABA, which relies on a monolayer of gold nanoparticles coated in silver [21], and an ultra-sensitive detection technique for ABA using SERS was discussed in [22]. Other

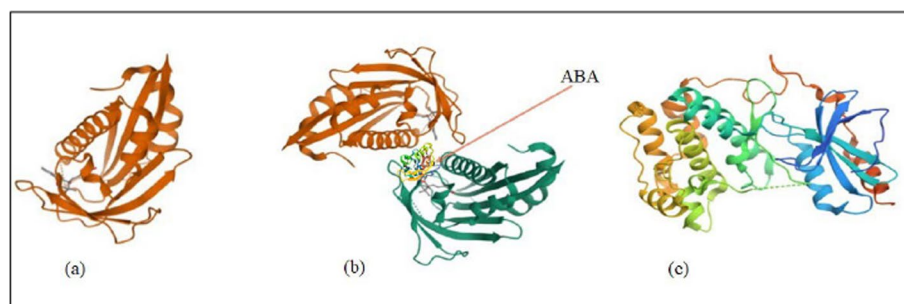


**Fig. 1** Structure of ABA-PYR1/PP2C interactions **a** golden PYR1 confirmation while **b** in green bounded with ABA and **c** ABA-PYR1/PP2C complex

techniques involved using dual-functional SERRS with a fluorescent aptamer sensor utilize charged gold nanorods [23], while biosensor development techniques using PYR/PYL receptor-based systems in yeast rely on plant-derived ABA sensing mechanisms [24]. These systems employ ABA-induced protein dimerization between PYR/PYL receptors and PP2C phosphatases to generate a detectable signal, such as fluorescence, enabling high-throughput screening and fine-tuned regulation in engineered strains. Current plant hormone detection methods are limited in their selectivity to identify particular hormones within specific plant tissues and during specific developmental stages. Remote sensing and precision agriculture technologies have been discussed in [25], but these methods require special control systems, high power consumption, and time-consuming procedures. Although, biosensors have made significant progress, most rely heavily on fluorescence-based readouts, which require external excitation and are susceptible to photobleaching, limiting their robustness and scalability in certain applications.

Inspired by the study of plant signaling and MC [3], a novel concept emerges amalgamating bacterial cells' innate communication strategies with plants' molecular-level communication mechanisms, thus birthing a novel communication paradigm. Current bacterial-based simulators excel in controlled lab settings, focusing on bioengineered entities aligned with traditional communication paradigms [26–28]. Our endeavor encompasses the internalization of *E. coli* bacteria within plants [29], harmonizing it with MC [7–9], and accentuating the engineering of plant-based communication. This research proposes a cost-effective biological sensor to detect plant stress hormones using engineered bacteria with self-propulsion, operating without external power. Central to this sensor is detecting abscisic acid (ABA), a critical molecule in plant stress regulation. Merging insights from myriad research fronts, we introduce bacterial-based molecular communication into crops, thereby devising biological sensors. Following, a comparison of existing techniques for detecting plant hormone ABA with the proposed sensor highlighting stating gaps in existing systems and the specific properties of sensor is presented in Table 1.

The envisioned sensors, outlined in Fig. 2, emanate from tailored modifications of genetically engineered bacterial cells [30–32], sensitizing them to ABA and enabling them to emit light upon ABA exposure. Our choice of the widely studied and easily manipulated *E. coli* as the reference organism for this sensor attests to its potential, typically 2  $\mu\text{m}$  long and 0.5  $\mu\text{m}$  wide. *E. coli*'s adaptability and ease of cultivation position it as an optimal choice [33]. *E. coli*'s capacity to act as an endophyte within plant tissues further underscores its utility, offering the potential to reside within plants without causing harm [34]. The proposed sensor will be able to detect ABA in diverse stress conditions, including drought and pathogen response, within a modeled response time of 431.52 s.

Our research leveraged MATLAB simulations to comprehend bacterial movement across distinct plant segments. Taking hydroponic tomato plant as model, these simulations are systematically divided into five discrete phases, i.e., bacterial diffusion within cell walls of plant root, examining bacterial diffusion through a tunnel-like shoot in the presence of advection, scrutinizing the diffusion of attractants within a leaf-like porous medium, exploring bacterial movement influenced by chemotactic signal concentration

**Table 1** Comparison of existing ABA detection techniques with proposed biosensor

Feature	Existing systems	Contributions of Our Work
Sensitivity and detection time	Limited sensitivity to low ABA concentrations  Detection times often exceed several minutes, especially under field conditions	Improved sensitivity to ABA-enriched regions through bacterial chemotactic simulation  Can achieved a faster response time of 431.52 s, addressing detection delays
Bacterial mobility	Restricted bacterial mobility in plant tissues; biosensors confined to static environments	Integration of chemotactic movement simulation to model bacterial behavior in dynamic plant environments
Power demands	High power requirements for fluorescence- and spectroscopy-based detection systems	Focused on approaches suitable for in planta applications, reducing reliance on external power
Mathematical modeling	Limited use of dynamic mathematical models for bacterial movement and interaction with attractants	First to utilize advection–diffusion equations and chemotaxis PDEs to predict bacterial movement and response times
Field applicability	Not practical for remote or in planta field applications due to complexity and power demands	Designed to function effectively in plant environments, enhancing usability in remote and field conditions
Cost and time	Creating samples and experimental chemicals repeatedly incurs higher costs	In contrast, the sensor, once developed, possesses self-replicating capabilities, significantly reducing both cost and time
Fluorescence and luminescence	Most existing biosensors utilize yeast, where genetically encoded (modified) circuits are designed to detect ABA via fluorescence. These systems require external excitation to produce a measurable signal	The proposed biosensor suggests engineering <i>E. coli</i> to trigger luminescence, enabling the generation of a quantifiable signal without the need for external excitation

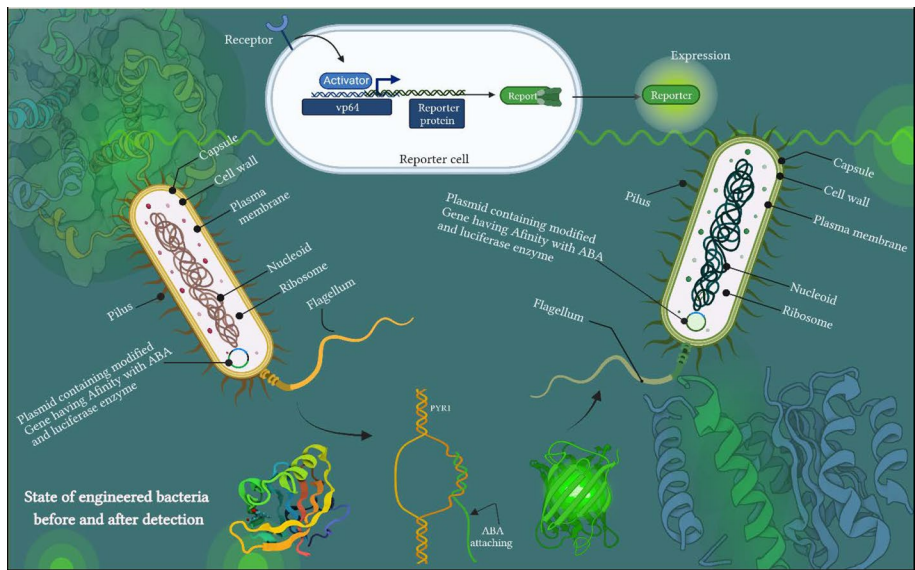


**Fig. 2** Proposed model of genetically engineered bacteria as a bioluminescent biological sensor, presenting its states before and after attachment of ABA

gradients, and simulating sensor's response time for detected hormone. Figure 3 encapsulates and visualizes these simulation phases. Figure 3a demonstrates the Transmission (Tx) process (bacterial internalization in plant roots), whereas Fig. 3b depicts the propagation in the channel (bacterial movement through plant shoot). Figure 3c shows the reception (Rx) at a desired location (bacteria's chemotactic behavior towards the attractant concentration).

### Design of proposed bacterial-based sensors

Genetically engineered bacteria (GEB) have been adapted to exhibit desired traits or functionalities, including sensing and responding to diverse stimuli [11–13]. Genetically engineered live cells can produce a physical signal responding to specific compounds or stress conditions [31]. This is achieved by fusing luciferase genes with target-activated promoters. When the target is present, it induces the promoter, leading to luciferase transcription and a dose-dependent luminescent signal [32]. For bacterial luciferase, the co-transcription of substrate-generating genes eliminates the need for external substrates. Bioluminescence as a reporter negates the necessity for an excitation light source, unlike fluorescence-based sensing [35, 36]. Building upon the innovative concept of bacterial-based biological sensors, the proposed model harnesses the remarkable capabilities of genetically engineered *E. coli* bacteria to function as highly sensitive detectors within the domain of plant biology. This novel sensor design capitalizes on the intricate interplay between molecular interactions and cellular processes, enabling the identification and response to specific analytes. In alignment with this exploration, our study introduces an innovative biological sensor model centered on the genetic

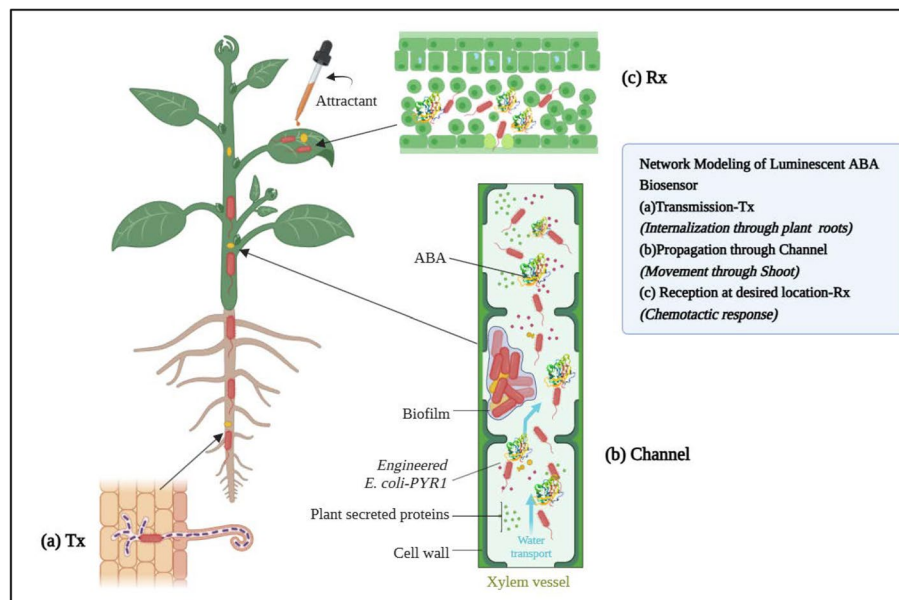


**Fig. 3** Schematic representation of the network modeling for a luminescent ABA biosensor system in plants. The model involves three key steps: **a** Transmission (Tx)—Internalization of engineered *E. coli* (PYR1) through plant roots facilitated by secreted proteins; **b** Propagation through Channel—Movement of biofilms and ABA (Abscic Acid) through xylem vessels, aided by water transport; **c** Reception (Rx)—Localization at the target site, where chemotactic response ensures desired biosensor functionality

manipulation of *E. coli* bacteria. One recent achievement in plant synthetic biology is the autonomous bioluminescence reporter system created by [37]. This approach allows for the reliable quantification of gene expression. This system does not require external luciferase substrates because it uses *Neonothopanus nambi*'s bioluminescence pathway. This makes it an economical option for processing multiple samples at once. The introduction of luciferase reporters controlled by stress-responsive promoters significantly improves the detection capabilities of ABA biosensors, as reported in "Ares genetic screening procedures" [38]. The evaluation and comparison of different reporter systems, including GUS, LUC, and GFP, are presented in [39], further emphasizing the importance of selecting the appropriate reporter system for specific applications to develop efficient ABA biosensors.

In our proposed model, *E. coli* bacteria are genetically modified to express a specialized protein with a distinct affinity for abscisic acid (ABA). This protein is then imbued with bioluminescent properties through the controlled activation of Lucifer molecules via quorum sensing mechanisms. The outcome is a modified *E. coli* strain that adeptly identifies ABA presence in plant organisms, promptly emitting a bioluminescent response. Our approach outlines a comprehensive sequence of steps for this achievement. To realize this vision, plasmids emerge as valuable vectors, serving to introduce genes responsible for ABA receptors and luciferase enzymes into the bacteria. Leveraging the inherent chemotactic behavior of bacteria, these modified *E. coli* strains autonomously gravitate toward ABA sources within plant tissues. A protein with high affinity and specificity for ABA, PYR1, a plant abscisic acid (ABA) receptor, has a malleable ligand-binding pocket, as discussed in [40] proposed for quickly creating biosensors that facilitate to enable the function of sense response. High-density mutagenesis of PYR1's has been used to create a library of stable double mutants, enabling the identification of more ligands. The ABA sensing system operates through a naturally occurring chemically induced dimerization (CID) mechanism where PYR1 recognizes the ligand, leading to the formation of a stable PYR1-ligand-protein phosphatase (PP2C) complex that inhibits phosphatase activity. The phosphatase acts as a coreceptor, lowering ligand off rates and boosting apparent affinity up to ~100-fold, enabling micromolar PYR1 ligand-binders to act as nanomolar sensors in the presence of phosphate. Different innovative design techniques, such as Rational Design [41] and De Novo Design [42], can be employed to identify nucleic acid sequences with robust ABA-binding capabilities. By binding to its intended target molecule, this protein enables the bacteria to sense and interact with the specified analyte effectively. Nature offers an array of luciferases and associated luciferins, bearing witness to the independent evolution of bioluminescence more than 40 times [43]. The genetic basis for this phenomenon is encoded within the lux operon, encompassing the luxCDABE genes. These genes orchestrate the synthesis of bioluminescent proteins and their accompanying substrates [44]. A quorum-dependent bioluminescent response can be achieved by harnessing quorum-sensing system genes, such as *luxI* and *luxR*. *LuxI* generates a signaling molecule, while *LuxR*, functioning as a transcriptional regulator, responds to the presence of this signal. The architecture of our system necessitates an intricate interplay, where the ABA-bound protein triggers the quorum sensing mechanism, ultimately inducing the activation of bioluminescent gene expression. The culmination of our proposed model involves the creation of a sophisticated genetic construct

encompassing the protein sequence, the quorum sensing apparatus, and the bioluminescence-related genes. This construct is meticulously tailored with appropriate promoters and regulatory components to ensure precise expression and regulation within *E. coli*. Facilitated by methods such as recombinant DNA technology [45], electroporation [46], or heat shock transformation [47], the genetic construct is seamlessly introduced into the *E. coli* strain. Following successful integration, rigorous experimentation can be undertaken to ascertain the modified bacteria's proficiency in ABA detection and subsequent bioluminescent response. The words 'biosensor' and 'bacterial' may be used interchangeably. The terms "engineered bacteria" and "modified bacteria" will be used interchangeably throughout the manuscript to convey the same meaning.

## Material and method

### Model for bacterial diffusion/internalization

This section discusses the simulation's analytic modeling, the diffusion equation, and advection, providing a comprehensive understanding of the processes involved. The supplementary material under supplementary Sect. 1 describes a fundamental approach adopted for bacterial diffusion in plants, including attractant diffusion and its impact on bacterial movement.

### Modeling the bacterial diffusion into plant root

The initial phase of our investigation employs a computational simulation to explore the diffusion and advection of engineered *E. coli*-PYR1 within a plant root cell, which is modeled to represent the root of a hydroponic plant. Bacterial internalization in hydroponic plant roots is a process by which bacteria penetrate the root surface and enter the root cells. This can occur through natural openings, such as root caps, lateral root emergence zones, root hairs, hydathodes, and mycorrhizal associations, or wounds caused by insects, animals, or mechanical damage [48]. Another hypothesis for its internalization is that it can naturally internalize into plant tissues in the rhizophagy process. Rhizophagy, or the "rhizophagy cycle," is a phenomenon by which plant roots cultivate bacteria on their root surface, internalize them into root cells, and extract nutrients from them by subjecting them to superoxide produced by root cells [49–52]. This process involves the participation of plant-derived cell wall degrading enzymes that loosen cell walls, allowing microbes to permeate plant root cells. Experimental studies with *Arabidopsis thaliana* and *Lycopersicon esculentum* inoculated with *E. coli* revealed heightened expression of cellulases in plants exposed to bacteria. The significance of this finding lies in the potential of cellulases to degrade cell walls, which could facilitate bacterial entry [49].

Once inside the plant cells, bacteria can become endophyte, microorganisms that live within plant tissues without causing apparent harm to the host. Endophytic bacteria can establish mutualistic, commensal, or pathogenic interactions with plants, depending on various factors such as bacterial strain, plant species, environmental conditions, and plant defense responses. Endophytic bacteria can also influence plant growth, development, nutrition, and stress tolerance by producing phytohormones, solubilizing phosphate, fixing nitrogen, producing siderophores, inducing systemic resistance, and degrading pollutants [53, 54].

*Escherichia coli* can also produce indole acetic acid (IAA), a phytohormone that can promote root development and growth [55]. As discussed earlier, it is generally considered that *E. coli* is a bacterium associated with animal microbiomes or a pathogen that causes foodborne diseases. According to a study, plants can establish symbiotic associations with *E. coli*, where the bacterium is internalized into seedling tissues. This may improve seedling development and nutrient status and protect plants from disease agents. These findings contradict the general assumption that *E. coli* is mainly an animal-associated symbiotic or pathogenic bacterium or simply a contaminant of crop plants [34]. The simulation setup for the engineered *E. coli*-PYR1 is delineated in supplementary Sect. 2 of the supplementary document.

#### **Role of advection on bacterial diffusion through the shoot (channel-like) of plant**

During the travel toward the different parts of the plant [29, 56], while sensing the ABA, this part of the simulation approximates the bacterial diffusion associated with advection through a one cm-long channel that we relate to the plant's shoot. In this part of the simulation, we add advection as an instantaneous factor of water uptake as xylem flow velocity 0.54 mm/s [57] by the plant during the running phase of bacteria that helps it to move from one point to another in less time and simulates the advection–diffusion of a concentration of *E. coli* in the channel-like shoot. The parameters defined at the beginning of the simulation code are:

$D$ : Diffusion coefficient of *E. coli* in the bulk fluid.

$v$ : Velocity of water in mm/s.

$\mathcal{L}$ : Channel Length in  $\mu$ meters.

$r$ : Channel Radius in  $\mu$ meters.

$v_e$ : Velocity of *E. coli* in  $\mu$ m/s.

Referring to Eq. (S-2), in supplementary document Sect. 2, the diffusion coefficient  $D$  can be assumed constant. Finally, we arrive at the simplified advection–diffusion equation for the given scenario:

$$\Delta C / \Delta t = D \cdot \left( \Delta^2 C_e / \Delta x^2 + \Delta^2 C_e / \Delta y^2 \right) - \left( v / v_e \right) \cdot \left( \Delta C_e / \Delta x \right) + v_{term} \cdot \left( \Delta C_e / \Delta x \right) \quad (1)$$

where  $C_e$ : *E. coli* concentration,  $t$ : time,  $D$ : diffusion coefficient of *E. coli*,  $x$ : distance along the channel,  $y$ : radial distance from the channel center,  $v$ : velocity of water in the channel,  $v_e$ : velocity of *E. coli*.

and

$$v_{term} = v \cdot (x / (\mathcal{L} / 2))$$

The discretized differential equation solved in the code using the finite difference method is provided in the supplementary document under Supplementary Sect. 3.

#### **Attractants' diffusion in leaf and chemotactic behavior of *E. coli* (Against spatially varying concentrations of attractant)**

The third part of the simulation involves modeling the spatially varying concentration of an attractant, such as aspartate, in a porous medium taken to a plant leaf and the

chemotactic behavior of *E. coli* in this domain. This is achieved by solving a partial differential equation (PDE). The simulation assumes a domain size of 60  $\mu\text{m}$  and a rate of attractant production  $Q = 10^{-11}$  mol/s. The initial condition posits a higher concentration of the attractant in the center of the domain. Other parameters incorporated in the model include the diffusion coefficient of the attractant and the bacterial speed. The simulation performs a diffusion process for aspartate, a well-known attractant for *E. coli*, by calculating an effective diffusion coefficient for the porous medium. This effective diffusion coefficient is a function of the medium's porosity, tortuosity, and constrictivity, and it is used to compute the concentration of attractant molecules at specific points within the porous medium, in this case, a leaf. The porosity ( $\epsilon$ ), tortuosity ( $\tau$ ), and constrictivity ( $\mathcal{C}$ ) of the porous medium were given constant values of 0.35, 2.11, and 1, respectively [58]. The diffusion coefficient of aspartate in water at 25°C is approximately  $7.32 \times 10^{-10}$  m<sup>2</sup>/s. However, within the porous medium, this diffusion coefficient is generally lower than its value in the bulk fluid due to the tortuous and constricted nature of the porous pathways, according to [59] and [60]. With these constants in place, the effective diffusion coefficient  $D_{\text{eff}}$ . The amount of attractant in the porous medium will be computed per Eq. (S-3) of the supplementary document Sect. (2).

$$D_{\text{eff}} = D_{\text{bulk}} \cdot (\epsilon/\tau) \cdot \mathcal{C} \quad (2)$$

where  $D_{\text{eff}}$ : the effective diffusion coefficient of aspartate in the porous medium (m<sup>2</sup>/s),  $D_{\text{bulk}}$ : the diffusion coefficient of aspartate in the bulk fluid (m<sup>2</sup>/s),  $\epsilon$ : the porosity of the porous medium,  $\tau$ : the tortuosity of the porous medium,  $\mathcal{C}$ : the constrictivity factor of the porous medium.

The PDE under consideration in this simulation is a convection–diffusion equation. This equation serves to model the spatiotemporal distribution of the attractant concentration within the domain, reflecting its distribution over space and time:

$$\Delta C / \Delta t = D_{\text{eff}} \cdot \Delta^2 C / \Delta x^2 - Q \quad (3)$$

where  $c$  is the concentration of the attractant, ' $t$ ' is time,  $D$  is the diffusion coefficient of the attractant,  $v$  is the velocity of the bacteria, and  $Q$  is the rate of attractant production. To simulate bacterial movement, the code considers two distinct phases, i.e., tumbling and running. The movement behavior is influenced by the attractant concentration gradient, wherein in the tumbling phase (0.75 s), *E. coli* does the random movement without responding to the attractant gradient. They move toward the attractant gradient during the running phase (1.25 s) [11].

### Sensor's response time

Biosensors, on the other hand, offer the potential for rapid, sensitive, and specific detection of detected enzymes (in our case, it is ABA) in real-time [61, 62]. The detection time indicates how quickly a sensor can respond to the presence of a target plant hormone (ABA in our case); rapid detection is crucial for decision-making and intervention. To explain the dynamics of a biosensor system, the mathematical model used is a set of ordinary differential equations (ODEs) [63]. Model parameters follow biological processes such as ABA production and degradation, receptor binding and

dissociation, mRNA and protein dynamics, and the final bioluminescence output. The model also includes stochastic variations and dependencies on environmental factors like temperature, pH, and ionic strength described in [31, 32, 37–39]. This approach is commonly used for modeling biochemical reaction networks and sensor systems. In addition to ODEs, we include the Hill equation [64, 65] in our model to incorporate nonlinear biological responses, which is critical for accurately describing the behavior of real biosensor systems. It strikes a nice compromise between simplicity and the ability to capture complicated biological events, making it an effective tool for biosensor modeling and design. Comprehensive mathematical modeling is presented in the supplementary document under Supplementary Sect. 4.

## Results and discussion

### Diffusion time of engineered *E. coli*-PYR1 for plant root

As delineated in Supplementary Section 2, the simulation begins with defining parameters such as diffusion coefficient, cell radius, growth rate, and temperature range depicted in Fig. 4. In this graphical representation, the x-axis signifies the time, showing how the bacterial position changes over time. The y-axis denotes atmospheric temperature, and the z-axis quantifies the bacterial position for engineered *E. coli*-PYR1 to traverse through the plant root cells. The z-axis also extends in both positive and negative directions, where the negative portion of the z-axis represents bacterial positions closer to the root surface. In contrast, the positive part represents positions farther away from the root surface.

Moreover, the simulation of bacteria diffusion was conducted by updating the bacteria's position based on a diffusion process, causing it to move randomly over time. The growth rate accounted for the bacteria's exponential growth. Temperature was randomly selected from a range, and the bacterial concentration was modeled using a diffusion equation that considered the position of the bacteria and time.

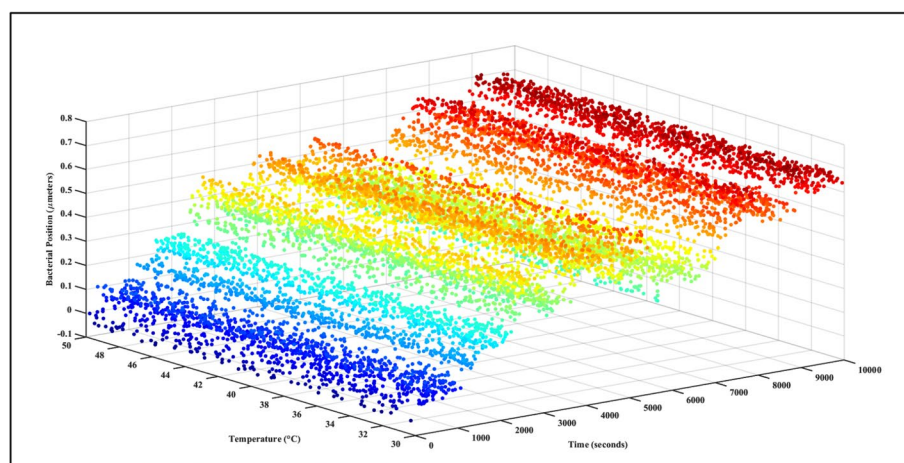


**Fig. 4** Illustrating the relationship between temperature and bacterial position. Each data point represents the position of the bacteria in plant roots under a randomly selected temperature condition, and the average time taken by Engineered *E. coli*-PYR1 is approximately 1220.12 s

Supplementary Figs. S1 and S2 highlight the correlation between temperature and position, bacteria's movement, and their concentration over time. Each data point on the plot of Fig. S1 represents a specific time instance, where the bacteria's position is plotted against the corresponding temperature. It can be noted that bacterial concentration is higher at higher temperatures. In Fig. S2a, we can observe the dynamic behavior of bacteria as they diffuse towards the plant root. The illustration shows the position of the bacteria changes over time due to the effects of diffusion. Bacteria tend to move randomly, resulting in a continuous change in their position. The positive bacterial position indicates concentration near the root cells, while the negative position indicates that the bacteria is away from the root. Figure S2b depicts bacterial concentration over time. Bacterial concentration increases exponentially as they undergo growth and proliferation. This growth is governed by the growth rate constant ( $k$ ), which represents the fraction of bacteria that divide and multiply per unit of time.

#### Effect of advection on engineered *E. coli*-PYR1 movement

A model presented in Fig. 5a demonstrates the diffusion of bacteria through the shoot. Shoot (Referred to as channel in the later discussion), with simulation results highlighting the significance of advection in the distribution and movement of *E. coli* within the

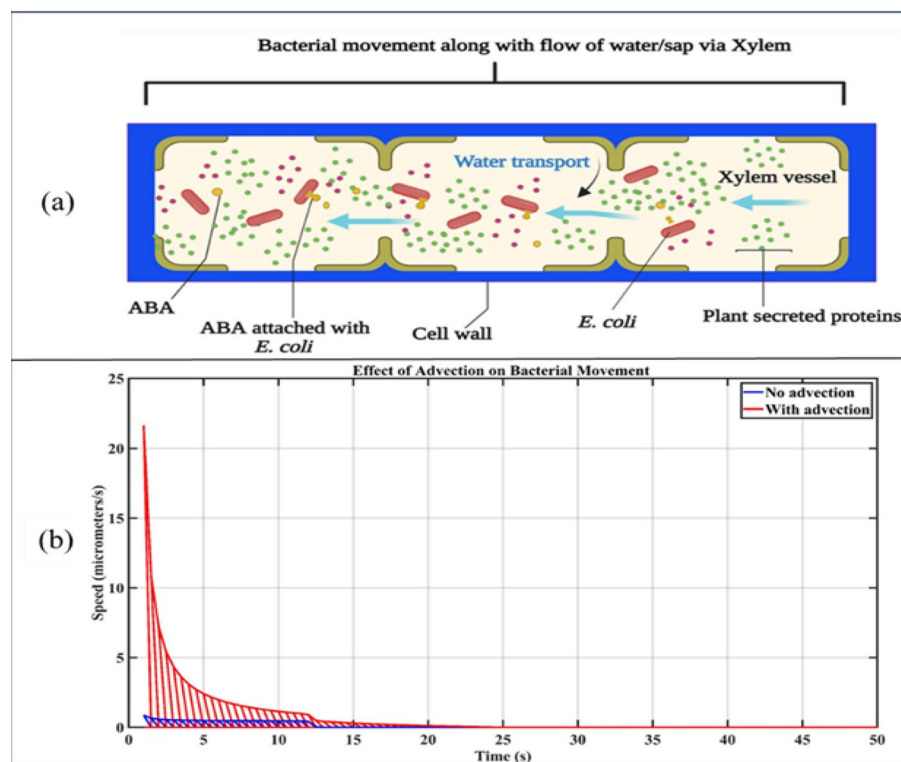


**Fig. 5** **a** Model of: A schematic representation of Engineered *E. coli*-PYR1 diffusion through the shoot in the xylem vessel of a plant. The diagram highlights the interaction between water/sap transport and bacterial dynamics. Bacteria move along the flow of water or sap within the xylem, encountering obstacles such as cell walls **b** Effect of advection on *E. coli*'s speed over time under two conditions: with advection (red line) and without advection (blue line). Advection notably increases the initial bacterial speed due to fluid flow in the xylem, with a sharp decay over time. In the absence of advection, bacterial movement relies solely on diffusion, resulting in consistently low speed throughout the time period

channel. The modeled simulation (“Role of advection on bacterial diffusion through the shoot (channel-like) of plant” Section) illustrates role of advection as it predominantly facilitates bacteria’s downstream movement and dispersion. In its absence, diffusion becomes the primary driver, resulting in a notably slower rate of bacterial spread. The consequential influence of advection on the bacteria’s velocity is further detailed in Fig. 5b. It can be observed that the presence of advection enhances the downstream spread and expedites the bacteria’s overall colonization of the channel, resulting in a marked increase in the bacteria’s spatial coverage and velocity within the channel.

Spatial and temporal variations refer to fluctuations in concentration distribution across locations and periods. Initially, diffusion regulates behavior, leading to homogenization. Over time, advection becomes significant, accelerating bacterial spread and expanding spatial coverage. The interaction between diffusion and advection shapes bacterial colonization and dispersion’s geographical and temporal patterns. Advection enhances velocity, while diffusion aids dispersion and blending. The simulation highlights the significance of incorporating advection factors into investigations about the motion and dispersion of *E. coli* or other microbes in plant shoots. Based on the study’s results, the graphic indicates that when exposed to advection, *E. coli* can reach a speed of 21.65  $\mu\text{m/s}$ , whereas it can only reach a speed of 0.866  $\mu\text{m/s}$  when advection is absent. The plot provides valuable information about the behavior of bacteria in constrained flow systems and emphasizes the critical role of advection in influencing bacterial motility.

#### Attractant diffusion and bacterial mobility concerning attractant concentration

The designed MATLAB code simulates and visualizes the dynamics of bacterial movement in response to an attractant concentration gradient. Supplementary Sect. 3.5 states that the value of the effective diffusion coefficient of the attractant for the porous medium is inversely proportional to the higher porosity, tortuosity, and constrictivity factors. Therefore, the factors mentioned above reduced the available pore space and increased the complexity of the pore geometry for diffusion. The diffusion coefficient of aspartate in water at 25°C is approximately  $7.32 \times 10^{-10} \text{ m}^2/\text{s}$ . To make our model more realistic, we consider the porosity, tortuosity, and constrictivity of the porous medium and the pore size as important components of our simulation [58]. Using Eq. (2) for aspartate and putting values of  $\varepsilon = 0.35$ ,  $\tau = 2.11$ , and  $\mathcal{C} = 1$  in it, we get

$$\mathcal{D}_{eff} = \left(7.32 \times 10^{-10}\right) \cdot \left[0.35/2.11 \cdot (1)\right]$$

The effective minimum value of the diffusion coefficient will be  $\mathcal{D}_{eff} = 1.2142 \times 10^{-10} \text{ m}^2/\text{s}$ , and for the  $\varepsilon = 0.45$ ,  $\tau = 2.77$  and  $\mathcal{C} = 3$ ,

$$\mathcal{D}_{eff} = \left(7.32 \times 10^{-10}\right) \cdot \left[0.45/2.77 \cdot (3)\right]$$

The effective maximum value of the diffusion coefficient will be  $\mathcal{D}_{eff} = 3.56 \times 10^{-10} \text{ m}^2/\text{s}$ .

Figure 6 effectively showcases the spatial and temporal distribution of the attractant concentration. The concentration of the attractant tends to increase around the middle. Over time, due to diffusion, this concentration spreads outward, reducing its intensity

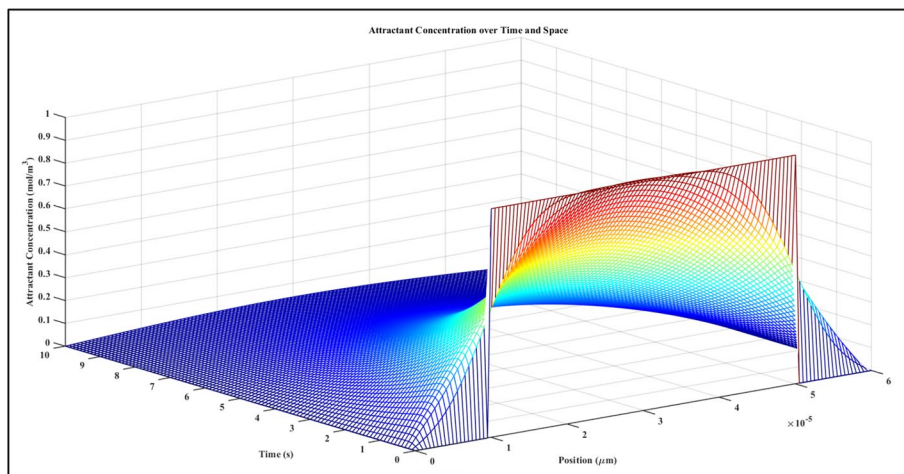


**Fig. 6** Attractant concentration over time and space

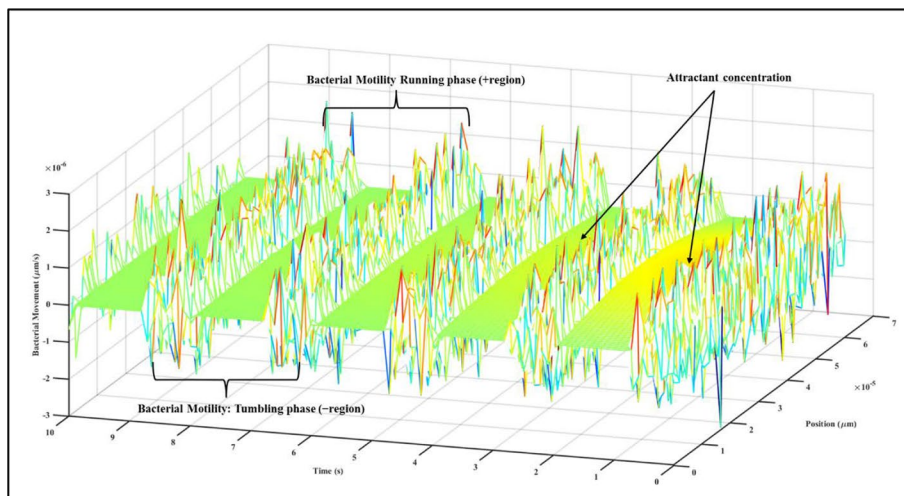


**Fig. 7** Engineered *E. coli*-PYR1 bacteria running/tumbling movement concerning attractant concentration

in the center and increasing towards the domain's edges. Showing this in a mesh grid is a graphical representation that depicts the concentration values at various points along the x-axis and times along the y-axis. The z-axis indicates the attractant's concentration, measured in units of moles per cubic meter (max  $1 \text{ mol/m}^3$  after 02 s). The contour lines superimposed on the surface offer supplementary understanding regarding the levels of concentration observed at different time intervals. The surface displays color variation corresponding to the attractant concentration degree.

Figure 7 illustrates the simulated locomotion patterns of *E. coli* bacteria in response to the spatial gradient of attractant concentration at a production rate of  $10^{-11} \text{ mol/s}$  within the domain of  $60 \text{ μm}$ . The observed lag in bacterial movement reveals that *E. coli* doesn't respond instantaneously to alterations in the attractant concentration. This delay implies the presence of internal processing or assessment phases within the bacteria, preceding adjustments to their locomotion. The bacterial motility is characterized by distinct

phases: a ‘tumbling’ phase, lasting approximately 0.75 s, and a ‘running’ phase, enduring for roughly 1.25 s. During the ‘running’ phase, the bacteria exhibit directional movement towards increasing attractant gradients, resulting in a more structured, linear motion pattern. In contrast, the ‘tumbling’ phase is marked by stochastic, non-linear movements, causing the bacteria to adopt more dispersed spatial arrangements. This phase introduces stochastic perturbations to bacterial motility.

Consequently, negative values on the z-axis within the mesh plot during the tumbling phase may indicate inherent irregularities in natural bacterial movement. In the context of this simulation, such negative values suggest movements of the bacteria in a direction opposing the gradient of the attractant concentration. In this framework, the mesh plot visually delineates the spatiotemporal patterns of *E. coli* movement, where the x-axis represents physical coordinates, the y-axis signifies time, and the z-axis quantifies the bacteria’s positional changes in response to the attractant gradient. After 2 s, the attractant was most concentrated at 1 mol/m<sup>3</sup>, and the calculated absolute distance covered by *E. coli* was 10 µm.

Figure S3 shows a scatter plot where each point represents the position of the engineered *E. coli*-PYR1 at a particular time. The color of each point indicates the attractant concentration at that position and time. Based on the defined parameters, the simulation shows that engineered *E. coli* PYR1 traveled approximately 4.76 µm from a lower to a higher attractant concentration at a calculated speed of  $1.0 \times 10^{-9}$  m/s over about 476s.

#### Response time for engineer *E. coli*-PYR1-biosensor

Our simulations capture several crucial characteristics in the setting of a biosensor, as described in “[Sensor’s response time](#)” Section and modeled in supplementary section 4. The sensor’s sensitivity is influenced by the binding kinetics of ABA and its receptor, a key parameter considered in the model. The total reaction time of the biosensor, defined by the sequence of events from ABA binding to bioluminescence production, highlights the intricate interplay of molecular events that can be tailored to specific applications.

For instance, in real-world agricultural scenarios, the detection of ABA—a key phytohormone regulating plant responses to water stress—has critical implications for drought-resilient crop management. By simulating how the biosensor responds to varying ABA concentrations, we provide insights into its potential application in monitoring water-stress levels in crops such as wheat, maize, and rice. An increase in the sensor’s detection limit, as suggested by the model, may enhance its utility for early-stage stress detection in plants under marginal drought conditions.

Furthermore, the model’s use of Hill equations to capture non-linear responses mirrors the behavior of actual biosensors, which can accommodate varying sensitivity levels under different physiological conditions. This approach also aids in optimizing the biosensor for specific stress scenarios, such as drought gradients in arid zones. For example, the surface mesh visualizations of detection times provide actionable data for selecting threshold bioluminescence intensities and initial ABA concentrations that correspond to faster detection in stressed crops. The shorter detection times (depicted in blue to green colors) can inform biosensor deployment strategies, such as real-time monitoring during critical growth stages.

By linking these findings to practical agricultural challenges, such as water-use efficiency or stress management in high-yielding crop species, our study establishes a robust framework for the translation of biosensor simulations into field-ready applications. By manipulating different factors within this mathematical framework, biosensor designs can be optimized to obtain certain performance features, such as lower detection limits, faster detection times, or greater specificity (Fig. 8).

### Comparative analysis of the simulation results with the experiment data

The proposed biological sensor model represents an innovative stride towards inexpensive, advanced sensing technologies. It involves engineering *E. coli* bacteria with receptors derived from PYR1, a plant ABA receptor. The detection system is coupled to a luciferase enzyme, which catalyzes a luminescence reaction when ABA binds to the receptors, thereby signaling the presence of ABA. Simulation models illustrate the proposed biosensor's capabilities in that it achieves an average response time of 431.52 s, which is in line with the experimental setup discussed in [31]. Further, the study [32], stated that amplification of the signal is required to lower the detection time of a whole cell biosensor. This implies that lower concentrations (near the detection limit) would require longer detection times [66]. The simulated results in Fig. 9 show the detection time against the different concentrations of ABA, aligned with the experimental data presented in the previous studies. At lower concentrations (near the detection limit), the detection time increases significantly, which are indicative of lower concentrations of the analyte (ABA). This is because lower luminescence outputs near the detection limit necessitate more time to achieve a measurable signal above the noise threshold.

The calculated time to traverse plant roots during the rhizophagy process is approximately 1220.12 s. We have modeled the impact of water flow in the xylem causes advection to increase bacterial movement up to 21.65  $\mu\text{m/s}$ , overcoming diffusion constraints in shoots is based on the studies of plants [29]. Referring to Fig. S3, our model

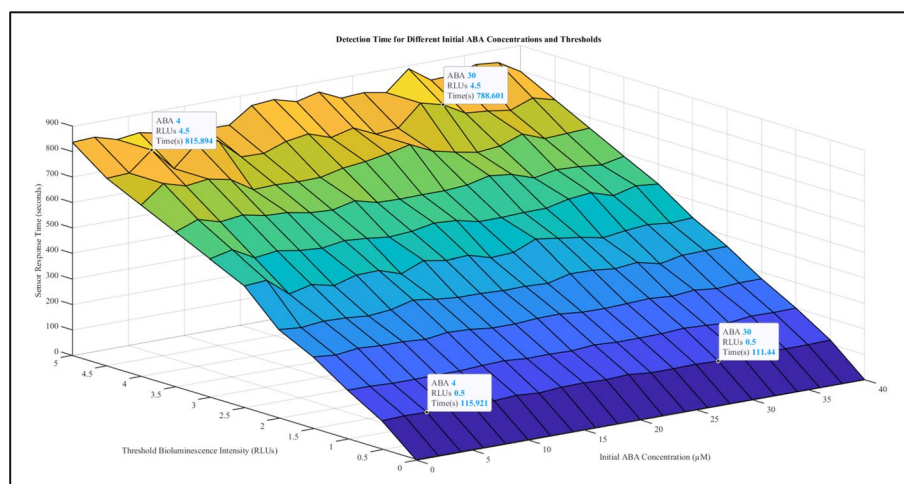


**Fig. 8** Engineered *E. coli*-PYR1 biosensor's response time calculation. 3D figures have been developed to understand the link between the higher time-dependent concentration of ABA and the response time. Lower detection time has been shown with the dark colors and vice versa. The average total time taken by bacteria to respond is calculated as 431.52 s

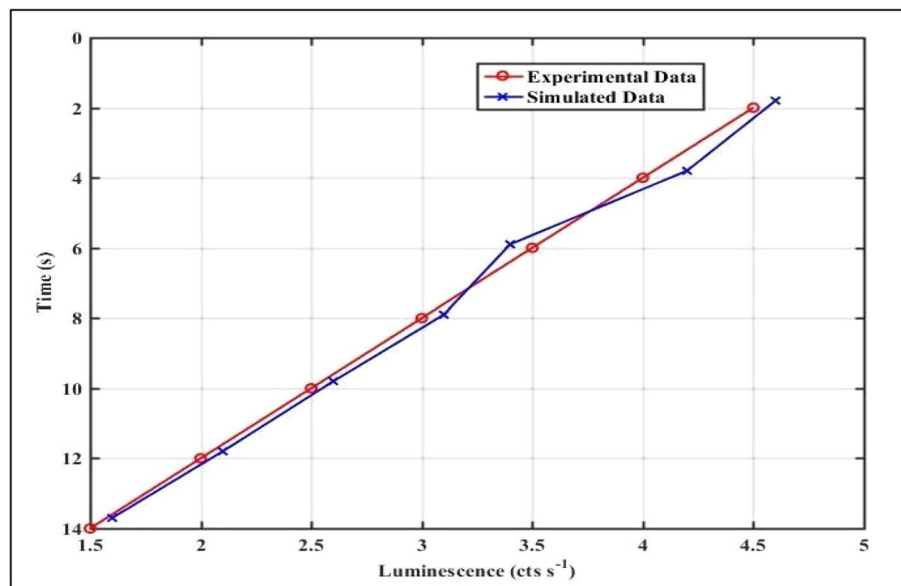


**Fig. 9** Comparison of the response time of the sensor against the different concentrations of ABA and with a whole cell heavy metal biosensor

incorporates not only the innate bacterial properties but also the environmental factors to simulate its behavior making our model more robust than presented in [11]. The simulated results exhibit sensor's chemotactic behavior in response to attractant concentration gradients in plant leaves, moving around  $4.76\mu\text{m}$  in response to different attractant levels, producing at a rate of  $10^{-11}$  mol/s and accomplishing this within an average time duration of 460 s. These techniques can be expanded to deploy multiple sensors for detecting various plant hormones, enhancing early stress detection and plant monitoring.

The biosensor's ability to monitor ABA levels provides practical applications in early detection of drought and salinity stress, enabling timely interventions and optimized irrigation strategies to reduce crop losses. The insights into detection times and bioluminescence thresholds offer precise, actionable data tailored to specific agricultural stress scenarios, making the biosensor a valuable tool for precision agriculture.

Incorporating deep learning and AI into biosensor design further enhances its potential by optimizing parameters such as binding kinetics and detection thresholds, enabling real-time adaptation to environmental changes. AI-driven predictive models support multi-analyte detection, while advanced techniques like reinforcement learning and generative adversarial networks (GANs) accelerate the discovery of novel designs and improve signal amplification. Integration with IoT platforms provides actionable insights for smart agriculture applications, including stress mitigation and precision irrigation.

## Conclusion

Our research proposes an innovative biological sensor for detecting plant hormones engineered to mitigate the stochastic behavior inherent in natural systems. The proposed biological sensor model represents an innovative stride towards inexpensive,

advanced sensing technologies. Our biological sensor model involves engineering *E. coli* bacteria with receptors derived from PYR1, a plant ABA receptor. The detection system is coupled to a luciferase enzyme, which catalyzes a luminescence reaction when ABA binds to the receptors, thereby signaling the presence of ABA.

Simulation models illustrate the sensor's capabilities as it achieves an average response time of 431.52 s and can traverse plant roots in approximately 1220.12 s during the rhizophagy process. Water flow in the xylem creates an advection that speeds up bacterial movement up to 21.65  $\mu\text{m/s}$ , overcoming diffusion constraints in shoots. Additionally, the bacteria exhibited chemotactic behavior in response to attractant concentration gradients in plant leaves, moving around 4.76  $\mu\text{m}$  in response to different attractant levels, producing at a rate of  $10^{-11}$  mol/s and accomplishing this within an average time of 460 s with speed of  $1.0 \times 10^{-9}$ . These techniques can be expanded to deploy multiple sensors for detecting various plant hormones, enhancing early stress detection and plant monitoring. This approach promises to improve agricultural management and resource efficiency significantly. Our ongoing efforts include leveraging deep learning and artificial neural networks to refine sensor design and deepen our understanding of ABA signaling. Collaborative efforts can further refine the design, leading to enhanced and reliable results through experimental validation and field implementation.

### Supplementary Information

The online version contains supplementary material available at <https://doi.org/10.1186/s12859-025-06082-8>.

Supplementary Material 1.

### Author contributions

Shakeel Ahmed: prepared and presented the work and wrote the original draft; Jiandong Hu: supervised, methodology, and conceptualized the work; Syed Muhammad Zaigham Abbas Naqvi and Muhammad Awais: data curation; Hao Zhang and Junfeng Wu: provided the study materials and maintained the research data; Linze Li: project administration; Vijaya Raghavan and Yongzhe Ren: View and editing.

### Funding

This work was supported by the National Key Technologies R & D Program of China during the 14th Five-Year Plan period (2021YFD1700904) and by the Major Science and Technology projects of Henan Province (221100320200) and supported by the Henan Center for Outstanding Overseas Scientists (GZS2021007).

### Availability of data and materials

All data and simulation files/codes are available online at Github under the link "<https://github.com/Shakeel-CN/E-coil-PYR1>".

### Declarations

#### Ethics approval and consent to participate

Not applicable.

#### Consent for publication

Not Applicable.

#### Competing interests

The authors declare no competing interests.

Received: 14 September 2024 Accepted: 12 February 2025

Published online: 25 February 2025

### References

1. Kranner I, Minibayeva FV, Beckett RP, Seal CE. What is stress? Concepts, definitions and applications in seed science. *New Phytol.* 2010;188:655–73.

2. Lee K, Missaoui A, Mahmud K, Presley H, Lonnee M. Interaction between grasses and *Epichloë* endophytes and its significance to biotic and abiotic stress tolerance and the rhizosphere. *Microorganisms*. 2021;9:2186.
3. Ahmed S, et al. Molecular communication network and its applications in crop sciences. *Planta*. 2022;255:128.
4. Santner A, Calderon-Villalobos LIA, Estelle M. Plant hormones are versatile chemical regulators of plant growth. *Nat Chem Biol*. 2009;5:301–7.
5. Wani SH, Kumar V, Shriram V, Sah SK. Phytohormones and their metabolic engineering for abiotic stress tolerance in crop plants. *Crop J*. 2016;4:162–76.
6. García-Andrade J, González B, Gonzalez-Guzman M, Rodriguez PL, Vera PJ. The role of ABA in plant immunity is mediated through the PYR1 receptor. *Int J Mol Sci*. 2020;21:5852.
7. Hiyama S, et al. Molecular communication. *J-Inst Electron Inf Commun Eng*. 2006;89:162.
8. Moore M, et al. Molecular communication: New paradigm for communication among nanoscale biological machines. *Handb Comput Netw: Distribut Netw Netw Plan Control Manag New Trends Appl*. 2007;3:1034–54.
9. Nakano T, Moore MJ, Wei F, Vasilakos AV, Shuai J. Molecular communication and networking: opportunities and challenges. *IEEE Trans Nanobiosci*. 2012;11:135–48.
10. Akan OB, Ramezani H, Khan T, Abbasi NA, Kusc M. Fundamentals of molecular information and communication science. *Proc IEEE*. 2016;105(2):306–18.
11. Cobo LC, Akyildiz IF. Bacteria-based communication in nanonetworks. *Nano Commun Netw*. 2010;1(4):244–56.
12. Unluturk BD, Bicen AO, Akyildiz IF. Genetically engineered bacteria-based biotransceivers for molecular communication. *IEEE Trans Commun*. 2015;63(4):1271–81.
13. Tsave O, et al. The anatomy of bacteria-inspired nanonetworks: molecular nanomachines in message dissemination. *J Nano Commun Netw*. 2019;21:100244.
14. Hirayama T, Mochida K. Plant hormonomics: a key tool for deep physiological phenotyping to improve crop productivity. *Plant Cell Physiol*. 2022;63(12):1826–39.
15. Westfall CS, Muehler AM, Jez JM. Enzyme action in the regulation of plant hormone responses. *J Biol Chem*. 2013;288:19304–11.
16. Gu Y-L, et al. *Pseudomonas* cyclic Lipopeptide medpeptin: biosynthesis and modulation of plant immunity. *Engineering*. 2023. <https://doi.org/10.1016/j.eng.2023.05.016>.
17. Ogundare SA, van Zyl WE. A review of cellulose-based substrates for SERS: fundamentals, design principles, applications. *Cellulose*. 2019;26:6489–528.
18. Nicolodelli G, Cabral J, Menegatti CR, Marangoni B, Senesi GS. Recent advances and future trends in LIBS applications to agricultural materials and their food derivatives: an overview of developments in the last decade (2010–2019). Part I. Soils and fertilizers. *TrAC Trends Anal Chem*. 2019;115:70–82. <https://doi.org/10.1016/j.trac.2019.03.032>.
19. Wang S, et al. Localized surface plasmon resonance-based abscisic acid biosensor using aptamer-functionalized gold nanoparticles. *PLoS ONE*. 2017;12:e0185530.
20. Roy M, Prasad A. Raman spectroscopy for nutritional stress detection in plant vascular tissue. *Materialia*. 2022;24:101474.
21. Zhang, Y. et al. In: International Conference on agri-photonics and smart agricultural sensing technologies (ICASAST 2022). SPIE, pp. 77–81.
22. Zhang Y, et al. Ultrasensitive detection of plant hormone abscisic acid-based surface-enhanced Raman spectroscopy aptamer sensor. *Anal Bioanal Chem*. 2022;414:2757–66. <https://doi.org/10.1007/s00216-022-03923-w>.
23. Wang Y, et al. Predation of the eggs and young larvae of *Spodoptera litura* by the third instar larvae of *Chrysopa formosa*. *Chin J Biol Control*. 2022;38:321.
24. Otto M, Dabirian Y, David F, Siewers, V. Sense and screen-ability: development of tuneable, biosensor-based screening platforms for abscisic acid. 2023.2005. 2016.540971 (2023).
25. Yang CJE. Remote sensing and precision agriculture technologies for crop disease detection and management with a practical application example. *Engineering*. 2020;6:528–32. <https://doi.org/10.1016/j.eng.2019.10.015>.
26. Bray D, Levin MD, Lipkow K. The chemotactic behavior of computer-based surrogate bacteria. *Curr Biol*. 2007;17(1):12–9.
27. Gregori M, Llatser I, Cabellos-Aparicio A, Alarcón E. Physical channel characterization for medium-range nanonetworks using flagellated bacteria. *Comput Netw*. 2011;55(3):779–91.
28. Vladimirov N, Løvdok L, Lebedz D, Sourjik V. Dependence of bacterial chemotaxis on gradient shape and adaptation rate. *PLoS Comput Biol*. 2008;4(12):e1000242.
29. Wright KM, et al. Differences in internalization and growth of *Escherichia coli* O157: H7 within the apoplast of edible plants, spinach and lettuce, compared with the model species *Nicotiana benthamiana*. *Microb Biotechnol*. 2017;10:555–69.
30. Liu Y, Feng J, Pan H, Zhang X, Zhang Y. Genetically engineered bacterium: Principles, practices, and prospects. *Front Microbiol*. 2022;13:4046.
31. Wen KY, Rutter JW, Barnes CP, Dekker L. In: Gerald Thouand, editors *Handbook of cell biosensors*, Springer International Publishing; 2019. pp. 1–23.
32. Chen S, Chen X, Su H, Guo M, Liu H. Advances in synthetic-biology-based whole-cell biosensors: principles, genetic modules, and applications in food safety. *Int J Mol Sci*. 2023. <https://doi.org/10.3390/ijms24097989>.
33. Ai Y, Sanders CK, Marrone BL. Separation of *Escherichia coli* bacteria from peripheral blood mononuclear cells using standing surface acoustic waves. *Anal Chem*. 2013;85:9126–34.
34. Verma SK, Chen Q, White JF. Evaluation of colonization and mutualistic endophytic symbiosis of *Escherichia coli* with tomato and Bermuda grass seedlings. *PeerJ*. 2022;10:e13879.
35. Williams CF, et al. Bioluminescence of *Vibrio fischeri*: bacteria respond quickly and sensitively to pulsed microwave electric (but not magnetic) fields. *J Biomed Opt*. 2019;24(5):051412–051412.
36. Strack R. Building up bioluminescence. *Nat Methods*. 2019;16(1):20–20.

37. Calvache C, Vazquez-Vilar M, Moreno-Giménez E, Orzaez D. A quantitative autonomous bioluminescence reporter system with a wide dynamic range for plant synthetic biology. *Plant Biotechnol J*. 2024;22:37–47. <https://doi.org/10.1111/pbi.14146>.
38. Chinnusamy V, Stevenson B, Lee BH, Zhu JK. Screening for gene regulation mutants by bioluminescence imaging. *Sci STKE: Sign Transduct Knowl Environ*. 2002;2002:140. <https://doi.org/10.1126/stke.2002.140.pl10>.
39. De Ruijter NCA, Verhees J, Van Leeuwen W, Van Der Krol AR. Evaluation and comparison of the GUS, LUC and GFP reporter system for gene expression studies in plants. *Plant Biol*. 2003;5(02):103–15.
40. Beltrán J, et al. Rapid biosensor development using plant hormone receptors as reprogrammable scaffolds. *Nat Biotechnol*. 2022;40(12):1855–61.
41. Pongsupasa V, Anuwat P, Maenpuen S, Wongnate T. Rational-design engineering to improve enzyme thermostability. *Enzyme Eng: Methods Protocols*. 2022. [https://doi.org/10.1007/978-1-0716-1826-4\\_9](https://doi.org/10.1007/978-1-0716-1826-4_9).
42. Gainza P, et al. De novo design of protein interactions with learned surface fingerprints. *Nature*. 2023;617(7959):176–84.
43. Gregor C, Gwosch KC, Sahl SJ, Hell SW. Strongly enhanced bacterial bioluminescence with the *ilux* operon for single-cell imaging. *Proc Natl Acad Sci*. 2018;115:962–7. <https://doi.org/10.1073/pnas.1715946115>.
44. Brodl E, Winkler A, Macheroux P. Molecular mechanisms of bacterial bioluminescence. *Comput Struct Biotechnol J*. 2018;16:551–64.
45. Bose R, Bose K. In: Textbook on cloning, expression and purification of recombinant proteins, Springer; 2022, pp. 1–12.
46. Cadoret F, Soscia C, Voulhoux R. Gene transfer: transformation/electroporation. *Pseudomonas Methods Protocols*. 2014. [https://doi.org/10.1007/978-1-4939-0473-0\\_2](https://doi.org/10.1007/978-1-4939-0473-0_2).
47. Froger A, Hall JE. Transformation of plasmid DNA into *E. coli* using the heat shock method. *J Vis Exp: JoVE*. 2007. <https://doi.org/10.3791/253-v>.
48. Moriarty MJ, Semmens K, Bissonnette GK, Jaczynski J. Internalization assessment of *E. coli* O157:H7 in hydroponically grown lettuce. *LWT*. 2019;100:183–8. <https://doi.org/10.1016/j.lwt.2018.10.060>.
49. Soares M, et al. Functional role of bacteria from invasive *Phragmites australis* in promotion of host growth. *Microb Ecol*. 2016;72:407–17.
50. White JF, Kingsley KL, Verma SK, Kowalski KP. Rhizophagy cycle: an oxidative process in plants for nutrient extraction from symbiotic microbes. *Microorganisms*. 2018;6(3):95.
51. Paungfoo-Lonhienne C, Schmidt S, Webb RI, Lonhienne TG. Rhizophagy: a new dimension of plant–microbe interactions. *Mol Microb Ecol Rhizosphere*. 2013;1:199–207.
52. Paungfoo-Lonhienne C, et al. Turning the table: plants consume microbes as a source of nutrients. *PLoS ONE*. 2010;5(7):e11915.
53. Hardoim PR, et al. The hidden world within plants: ecological and evolutionary considerations for defining functioning of microbial endophytes. *Microbiol Mol Biol reviews*. 2015;79(3):293–320.
54. Santoyo G, Moreno-Hagelsieb G, del Carmen Orozco-Mosqueda M, Glick BR. Plant growth-promoting bacterial endophytes. *Microbiol Res*. 2016;183:92–9.
55. Teng K et al. Heterologous expression of a novel *Zoysia japonica* C2H2 zinc finger gene, *ZjZFN1*, improved salt tolerance in *Arabidopsis* 2018; 9:1159.
56. Selmi M, Gazzah MH, Belmabrouk H. Optimization of microfluidic biosensor efficiency by means of fluid flow engineering. *Sci Rep*. 2017;7:5721. <https://doi.org/10.1038/s41598-017-06204-0>.
57. Windt CW, Vergeldt FJ, De Jager PA, Van As H. MRI of long-distance water transport: a comparison of the phloem and xylem flow characteristics and dynamics in poplar, castor bean, tomato and tobacco. *Plant Cell Environ*. 2006;29(9):1715–29.
58. Lee SJ, Kim K, Ahn S. The internal structure of macroporous membranes and transport of surface-modified nanoparticles. *Microscopy Microanal*. 2015;21:936–45.
59. Tartakovsky DM, Dentz M. Diffusion in porous media: phenomena and mechanisms. *Transp Porous Med*. 2019;130:105–27.
60. Zech A, de Winter M. A probabilistic formulation of the diffusion coefficient in porous media as function of porosity. *Transp Porous Med*. 2023;146:475–92.
61. Dyussembayev K, et al. Biosensor technologies for early detection and quantification of plant pathogens. *Front Chem*. 2021;9:636245. <https://doi.org/10.3389/fchem.2021.636245>.
62. Narang J, Mohan H. Biosensors for phytohormone abscisic acid and its role in humans: a review. *Sens Int*. 2023;4:100234.
63. Ndathe R, Dale R, Kato N. Dynamic modeling of ABA-dependent expression of the *arabidopsis* RD29A gene. *Front Plant Sci*. 2022;13:928718. <https://doi.org/10.3389/fpls.2022.928718>.
64. Lolkema JS, Slotboom DJ. The Hill analysis and co-ion-driven transporter kinetics. *J Gen Physiol*. 2015;145:565–74. <https://doi.org/10.1085/jgp.201411332>.
65. Weiss JNJTFJ. The Hill equation revisited: uses and misuses. *FASEB J*. 1997;11:835–41.
66. Duval JFL, Pagnout C. Decoding the time-dependent response of bioluminescent metal-detecting whole-cell bacterial sensors. *ACS Sens*. 2019;4:1373–83. <https://doi.org/10.1021/acssensors.9b00349>.

## Publisher's Note

Springer Nature remains neutral with regard to jurisdictional claims in published maps and institutional affiliations.